Capacitively-Excited Single-phase Asynchronous Generator for Autonomous Applications

K. A. Sanusi[1,*], L. Olatomiwa[2], A. D. Mohammed[1], K. A. Sodiq[3]

[1]Department of Electrical Engineering, Waziri Umaru Federal Polytechnic, Birnin Kebbi, Nigeria
[2]Department of Electrical & Electronic Engineering, Federal University of Technology, Minna, Nigeria
[3]Department of Computer Engineering, Yaba College of Technology, Lagos, Nigeria

ABSTRACT: The need to decentralize power generation and decarbonize the earth in order to have a sustainable global economy are the major reasons for the development of this paper. Considering the flaws of grid-connected power system, the autonomous system becomes a better alternative in rural and isolated areas. Analysis of stand-alone single-phase Asynchronous generator based on d-q model in a stationary reference frame is presented. Asynchronous generator does not have the capability to produce reactive power necessary for excitation and this must be provided by external means. Capacitive method has been considered in this paper due to its simplicity and its economic viability. The effects of magnetic saturation in the airgap has been considered by using the nonlinear relationship between the magnetizing inductance and the magnetizing current of the machine. Under this approach, the mutual inductance varies continuously. The results have shown that steady state condition of the generated voltage is not fixed but depends on the suitable combination of excitation capacitance and the rotor speed.

KEYWORDS: Self-excited induction generator, Remnant magnetic flux, Capacitive Excitation, Magnetic saturation, Steady state, Reference frame theory.

[Received Nov. 30, 2021; Revised Mar. 16, 2022; Accepted Mar. 22, 2022] Print ISSN: 0189-9546 | Online ISSN: 2437-2110

I. INTRODUCTION

In modern society, it is difficult to imagine life without electricity. In the nearest future, it is well anticipated that the present complex and traditional forms of energy generation would be completely phased out and be replaced with a more form of sustainable energy. The global energy sector is on the path of serious transformation and the focus can be described with single phrase - the 4th "energy transition" i.e from the conventional (centralized) form of energy systems of the 20th century to 3Ds (decarbonization, digitalization, decentralization) technology of the 21st century (Starkova *et al*., 2021).

Autonomous applications become a better alternative where the cost of grid extension is excessively high or where the transmission lines have to pass through thick bushes where the security cannot be guaranteed. In addition, it provides a quite appealing solution to access energy with a reasonable monthly billing unlike grid connected system where customers are additionally sub-charged with the cost of grid maintenance. Autonomous systems are also free from challenges like islanding detection, complex control system to achieve constant voltage and frequency which are faced by grid systems (Wang & Ossart, 2019).

However, self-excited induction generator (SEIG) has received enormous attentions in the recent past owing to its robustness nature. It is mostly deployed in fixed speed wind power plants and micro-hydro installations for autonomous or microgrid applications in far-off secluded places. Self-excited induction generators are widely used because of their simplicity, reduced cost, less maintenance, natural protection to short-circuit (Wang & Madawala, 2021; Wu *et al*., 2011), and they operate smoothly without hunting. SEIG is a better synchronous generator for slight load capability when connected to utility grid and equipped with dedicated controller for frequency and voltage compensation. The machine will then outputs voltage and frequency of appropriate value (Velmurugan *et al*., 2021).

Generally, squirrel cage induction generators (SCIG) are not self-exciting, they require external energy for the excitation of rotating magnetic field, either from the power grid or from static Vars sources such as capacitors, Interior Permanent Magnet (IPM) and pulse width modulation-based converters. Induction generators with the latter form of excitations are called autonomous induction generators, and apart from excitations they can also be used for voltage control (Ion and Syed, 2001).

Relative to three phase self-excited induction generator, little research attention has been given to single phase type and the very few literatures on single phase dwelled more on maximum and minimum capacitance requirements for self-excitation process (Mahato *et al*., 2006, Goyal and Palwalia, 2016, Silva *et al*., 2020). In (Debta & Mohanty, 2010; Ofualagba & Ubeku, 2011). Capacitive excitation of SCIG was treated but no explicit information was given on how the inherent remnant magnetic flux could be incorporated in the machine for voltage build up process. In this paper, transient and

*Corresponding author: kamilu.sanusi@tu-clausthal.de
doi: http://dx.doi.org/10.4314/njtd.v19i2.4

steady-state analysis of single phase SCIG is adequately treated with capacitive excitations suitable for single phase load in rural autonomous application.

Capacitive excitation is simpler and cheaper and those are the reasons for its popularity and most importantly its consideration in this paper. Saturation effects are considered in this paper by using the nonlinear relationship between the magnetizing inductance and the magnetizing current of the machine. Under this approach, the mutual inductance varies continuously. Dynamic model of Asynchronous generator (AG) on no load based on d-q model in a stationary reference frame is established and used in analyzing the transient and stability situations and making other predictions based on its characteristics.

II. CAPACITIVE EXCITATION OF SINGLE-PHASE INDUCTION GENERATOR

Bassett and potter in 1935 investigated and showed that induction machines can be operated as independent or isolated generators at pre-determined voltage and frequency by means of capacitive excitation (Bassett & Potter, 1935). Excitation capacitors could be on the stator or rotor of the generator, but on the stator is preferred because the stator terminals of the generator are easily accessible. In a three-phase machine, each phase is shunted with an appropriate valued capacitor. In a single-phase SEIG, one capacitor (C_d) is connected across the auxiliary winding to provide the required self-excitation, and another capacitor (C_q) in series or parallel with the main winding/load impedance to provide the voltage regulation and also aids in self-excitations. Among many possible configurations investigated by many researchers, Figure 1 holds a higher degree of generality in its analysis and seems very practical at the same time (Ojo & Bhat).

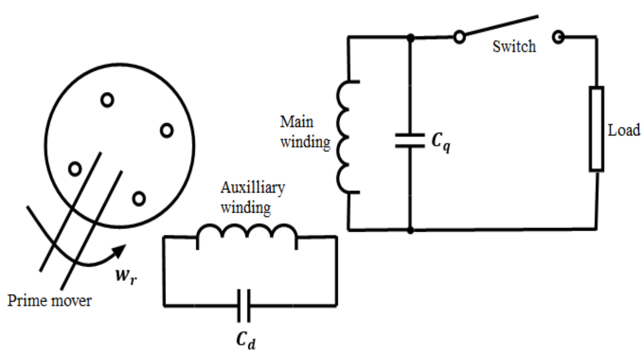

Figure 1: Schematic diagram of a capacitive excited and self-regulated induction single-phase generator.

III. MAGNETIC SATURATION AND VOLTAGE BUILD UP CHARACTERISTICS IN SEIG

A SEIG with an appropriate capacitor connected across its stator and propelled by a prime mover (e.g wind turbine) would initiate voltage build up at a suitable speed. It is important to know it is impossible for self-excitation process to be initiated in SEIG without the presence of residual magnetic flux in the core. The remnant flux could be inherent in the machine or as a result of previous operating condition. If machine loses its magnetism completely which is very unusual then it can be re-compensated by any of these processes; (i) pre-exciting the generator with DC or by employing a charged capacitor (ii) by keeping the rotor rotating for some time with the machine in a no-load condition (Simões and Farret, 2014, Grantham *et al*., 1989). The residual flux sets-up a small voltage in the stator which is applied to the capacitor that produces a lagging capacitive current which flow through the stator. This current will cause an increase in the air-gap flux which will also results in higher voltage that provokes a higher increase of the capacitive current.

This continues until the core is saturated, at this point voltage oscillating at a particular frequency and magnitude (at steady state) is generated. The magnitude of this terminal voltage is dependent on the saturation curve of a particular machine (i.e quality of the iron, core dimensions, overall geometry, coil windings). The saturation curve is often represented either by a polynomial or a nonlinear expression as given by (16) (Bassett and Potter, 1935, Simões and Farret, 2014, Al-Senaidi *et al*., 2021). As shown in Figure 2, excitation capacitance required is determined for a particular rotation in such a manner that the straight line of the capacitive reactance intercepts the saturation curve at the point of the desired rated voltage (V_t) (Debta & Mohanty, 2010).

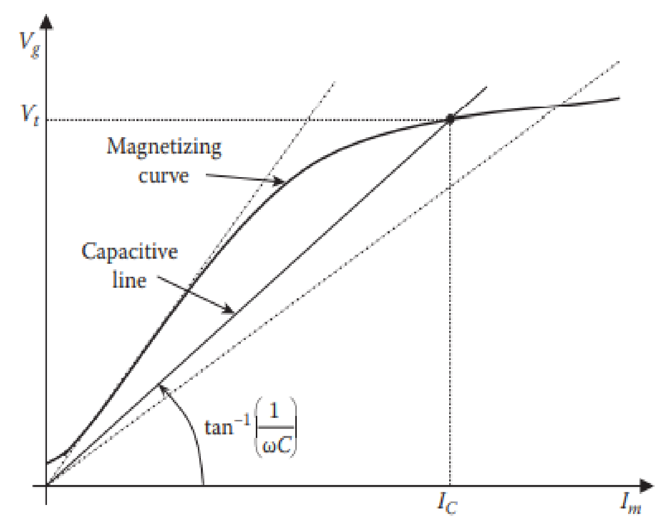

Figure 2: Saturation curve of Induction generator (Simoes and Farret, 2007)

IV. EFFECTS OF MAGNETIZING INDUCTANCE ON EXCITATION AND VOLTAGE STABILITY

In order to simulate SEIG, a non-linear equation that represent the characteristics of magnetizing inductance must be established. One very important ingredient that is very crucial to voltage buildup and its stabilization is the manner in which magnetizing inductance varies with time. At the start of excitation (point A), there is a finite value of magnetizing inductance in the core even when the phase voltage is zero as depicted in Figure 3. Once the self-excitation begins, phase voltage rises and magnetizing inductance also rises. Between point B and C, the magnetizing inductance begins to fall with rise in phase voltage until steady state is achieved.

Region AB is volatile, if SEIG begins to generate in this region, any decline in speed will result in corresponding decline in phase voltage which will in turn reduces L_m and finally voltage will collapse to zero. Once voltage falls to zero, there is no transient and there can't be voltage build up even if the speed once again increases to its initial value. This situation can lead to demagnetization of the core. Between point B and C is a stable operating region. When the speed decreases voltage will reduce and L_m increases as to ensure SEIG continues to operate at a lower stable voltage (Seyoum and Rahman, 2002).

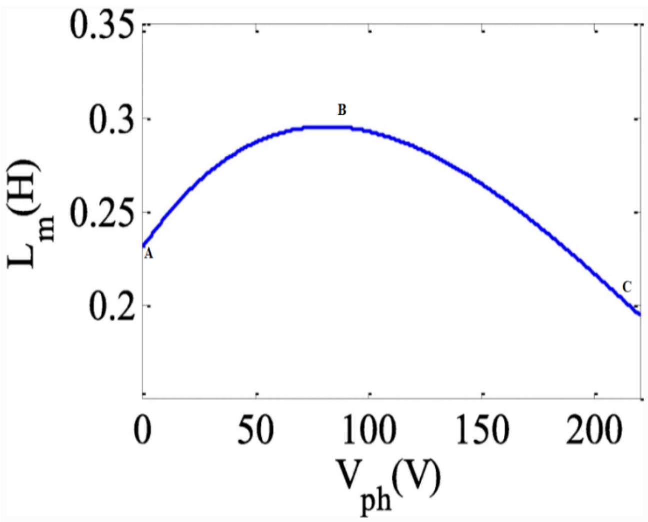

Figure 3: Saturation curve of Induction generator(Bendjeddou *et al*., 2021).

V. DYNAMIC MODELING OF SEIG USING REFERENCE FRAME THEORY

For the purpose of simplification in the analysis, the following assumptions have been made; (i) stator and rotor leakage inductances are assumed to be constant (ii) the air gap magnetomotive force (MMF) is sinusoidal (iii) The core losses represented by core resistors and shunted across the magnetizing branches is neglected (Ojo and Bhat, 1995). The model of SEIG is presented using d-q model in arbitrary reference frame. The direct-quadrature (d-q) model is very effective in analyzing the transient and steady state conditions of any system dynamics with reduced number of computations and with complete solutions (Seyoum, 2003). The classical representation of induction machine is shown in Figure 4 while the equivalent circuit on no load situation is shown in Figure 5. The classical d-q model of SEIG typically constitutes three sets of equations; voltage equations, flux equations, and motion equation.

The expression of these equations in an arbitrary reference frame are derived as follows;

Voltage Equations:

$$V_{qs} = i_{qs}r_s + p\lambda_{qs} + w\lambda_{ds} \quad (1)$$

$$V_{ds} = i_{ds}r_s + p\lambda_{ds} - w\lambda_{qs} \quad (2)$$

$$V_{qr} = i_{qr}r_r + p\lambda_{qr} + (w - \omega_r)\lambda_{dr} \quad (3)$$

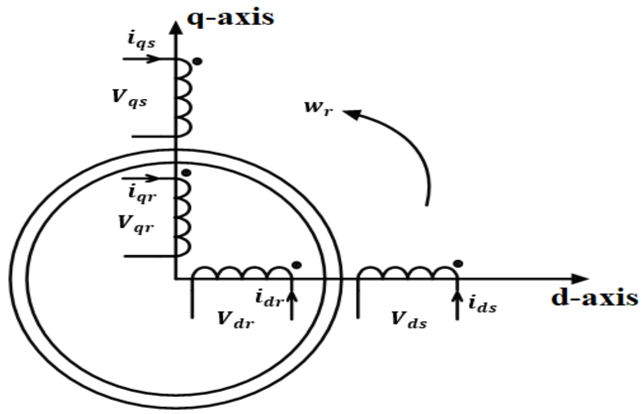

Figure 4: d-q representation of induction machine.

$$V_{dr} = i_{dr}r_r + p\lambda_{dr} - (w - \omega_r)\lambda_{qr} \quad (4)$$

d-q flux linkages:

$$\lambda_{qs} = L_s i_{qs} + L_m i_{qr} \quad (5)$$

$$\lambda_{ds} = L_s i_{ds} + L_m i_{dr} \quad (6)$$

$$\lambda_{qr} = L_r i_{qr} + L_m i_{qs} \quad (7)$$

$$\lambda_{dr} = L_r i_{dr} + L_m i_{ds} \quad (8)$$

where;

$$\begin{cases} L_s = L_{ls} + L_m \\ L_r = L_{lr} + L_m \end{cases} \quad (9)$$

The motion equation which describes the dynamic behavior of the rotor's speed in terms of mechanical and electromagnetic torques is given in Eqn. (10).

$$\frac{2J}{P} pw_r = T_L - T_e \quad (10)$$

$$T_e = \frac{3PL_m}{2}\left(i_{qs}i_{dr} - i_s i_{qr}\right) \quad (11)$$

Considering the initial conditions, the following equations are established;

$$\begin{cases} V_{qsc} = \frac{1}{C_q}\int i_{qs}\,dt + V_{qsc0} \\ V_{dsc} = \frac{1}{C_d}\int i_{qs}\,dt + V_{dsc0} \end{cases} \quad (12)$$

$$\begin{cases} w_r\lambda_{qr} = \left(L_r i_{qr} + L_m i_{qs}\right) + K_{qr} \\ w_r\lambda_{dr} = \left(L_r i_{dr} + L_m i_{ds}\right) + K_{dr} \end{cases} \quad (13)$$

where; K_{dr} *and* K_{qr} are the initial rotational induced voltage along the q and d axis respectively due to the remnant magnetic flux to derive d-q model of SEIG in synchronous reference frame or stationary reference frame, w in the voltage equations is set to w_s and 0 respectively. Stationary reference frame is considered for the analysis in this paper. Also, since the rotor is short-circuited, it means$V_{dr} = V_{qr} = 0$. By also considering Eqn. (13), Eqns. (1-4) can be formulated in a state space form as in Eqn. (14).

$$\begin{bmatrix} L_s & 0 & L_m & 0 \\ 0 & L_s & 0 & L_m \\ L_m & 0 & L_r & 0 \\ 0 & L_m & 0 & L_r \end{bmatrix} \begin{bmatrix} pi_{qs} \\ pi_{ds} \\ pi_{qr} \\ pi_{dr} \end{bmatrix} + \begin{bmatrix} r_s & 0 & 0 & 0 \\ 0 & r_s & 0 & 0 \\ 0 & -w_rL_m & r_r & -w_rL_r \\ w_rL_m & 0 & w_rL_r & r_r \end{bmatrix} \begin{bmatrix} i_{qs} \\ i_{ds} \\ i_{qr} \\ i_{dr} \end{bmatrix} + \begin{bmatrix} V_{qsc} \\ V_{dsc} \\ K_{qr} \\ K_{dr} \end{bmatrix} \quad (14)$$

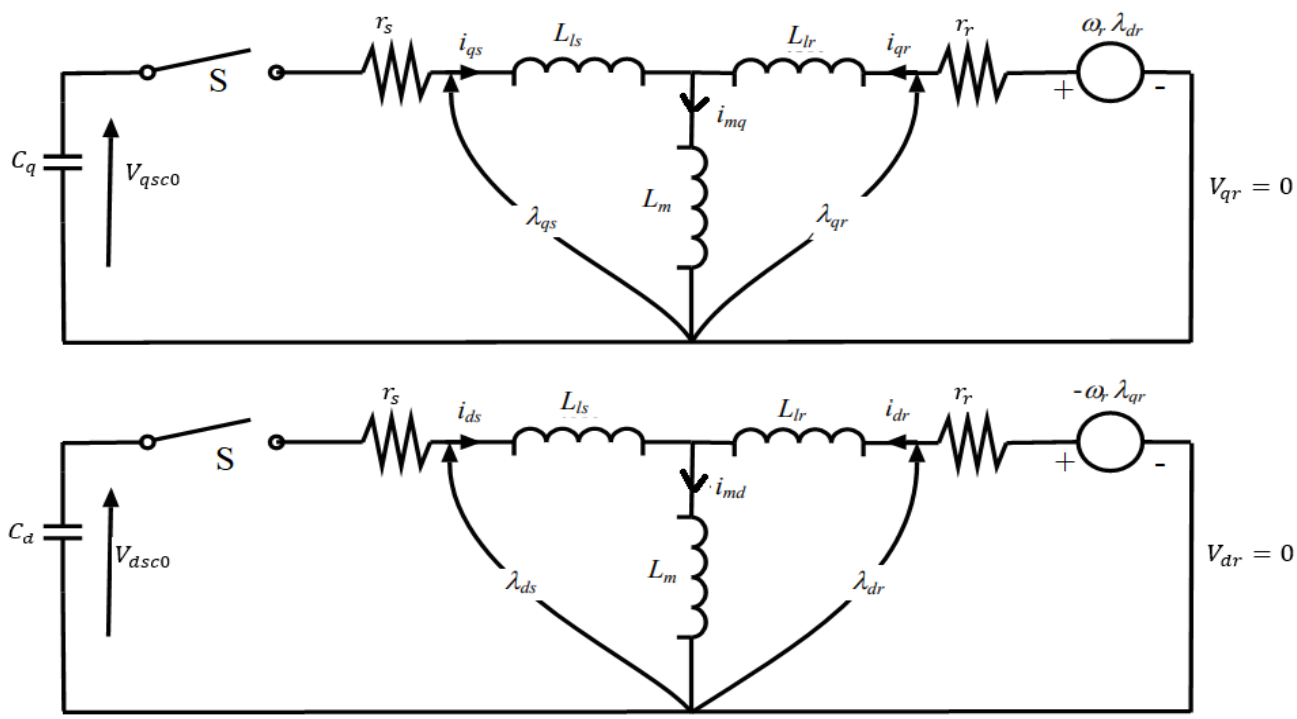

Figure 5: Equivalent circuit of capacitive SEIG.

The matrix of the current vectors derivatives is obtained and given in Eqn. (15).

$$\begin{bmatrix} pi_{qs} \\ pi_{ds} \\ pi_{qr} \\ pi_{dr} \end{bmatrix} = \frac{1}{L_r L_s - L_m^2}\left(\begin{bmatrix} -L_r r_s & -L_m^2 w_r & L_m r_r & -w_r L_m L_r \\ L_m^2 w_r & -L_s r_s & w_r L_m L_r & L_m r_r \\ L_m r_s & w_r L_m L_s & -L_s r_r & w_r L_s L_r \\ -w_r L_m L_s & L_m r_s & -w_r L_r L_s & -L_s r_r \end{bmatrix}\begin{bmatrix} i_{qs} \\ i_{ds} \\ i_{qr} \\ i_{dr} \end{bmatrix} + \begin{bmatrix} L_m K_{qr} - L_r V_{qsc} \\ L_m K_{dr} - L_r V_{dsc} \\ L_m V_{qsc} - L_s K_{qr} \\ L_m V_{dsc} - L_r K_{dr} \end{bmatrix}\right) \tag{15}$$

Using least square curve fit, the magnetizing inductance L_m is expressed as a function of the magnetizing current I_m and given in Eqn.(16) (Simoes and Farret, 2007);

$$L_m = 0.423e^{-0.0035 i_m^2} + 0.0236 \tag{16}$$

It is obvious from Figure 2 that the magnetizing curve of SEIG is nonlinear caused by saturation of the core, therefore L_m is not constant but rather depends on the instantaneous value of the magnetizing current i_m, which is evaluated in each step of the integration and given in Eqn. (17) (Mahato *et al.*, 2013)

$$i_m = \sqrt{\frac{(i_{ds}+i_{dr})^2 + (i_{qs}+i_{qr})^2}{2}} \tag{17}$$

VI. SIMULATION, RESULTS AND DISCUSSION

The simulation was carried out using MATLAB/ SIMULINK software, version R2020b with an empty charge on the capacitor. An impulse signal whose value fades away as soon as the first iteration is made was used to represent the remnant magnetic flux in the core for the initiation of excitation and subsequent voltage build up in the SEIG. A constant speed w_r of 250 rad/sec was initially used to simulate the system in the absence of prime mover model at capacitor value of 180uF. The simulation model diagram is as given in Figure 6.

Figure 7 shows the transient and the steady state behavior of the stator voltage and stator current with the machine speed on no load. Figure 8 illustrates the responses of magnetizing current and magnetizing inductance. It is obvious from the responses that the magnetizing inductance was at maximum at the beginning of excitation process, its value started dropping as soon as the machine started voltage build up. In a reverse manner, magnetizing current started from zero and also continues to build up as a result of continuous iteration until magnetic core become saturated.

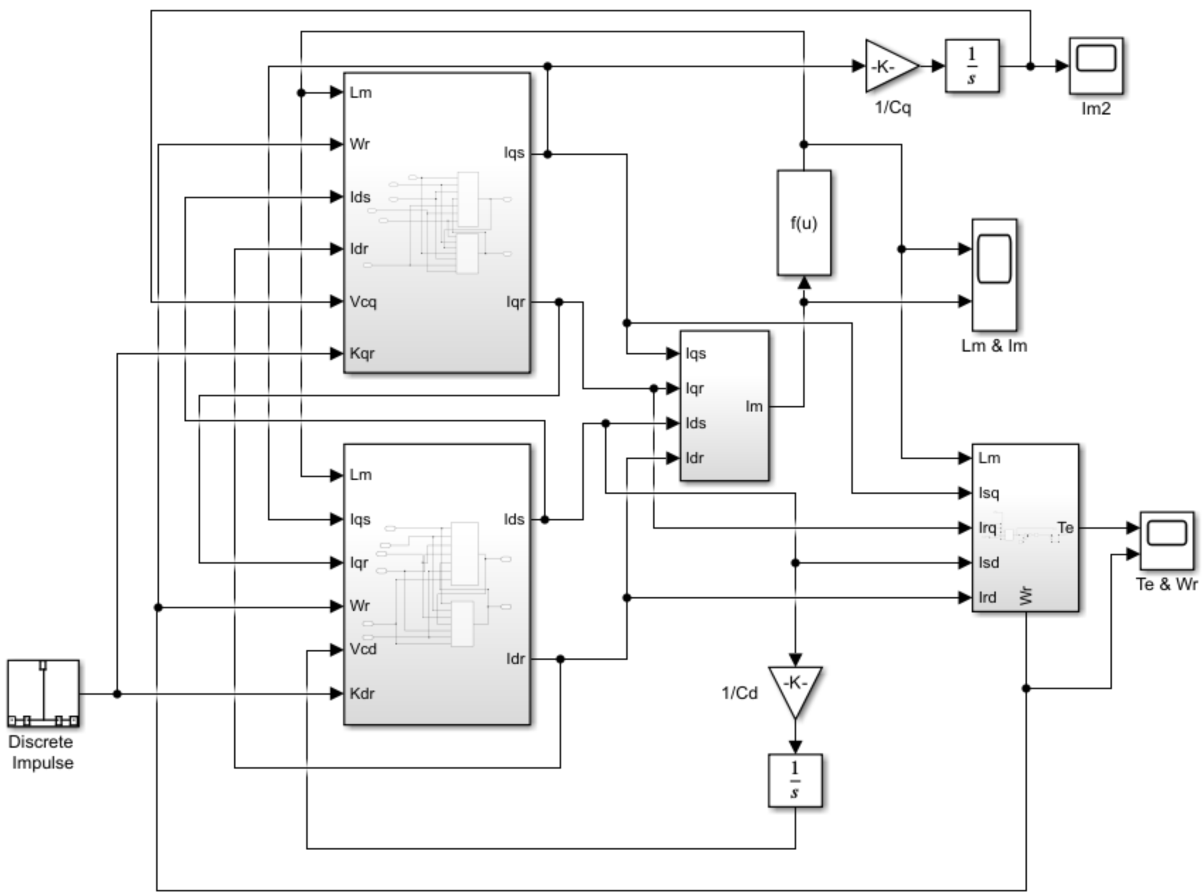

Figure 6: Simulation model diagram of SCIG.

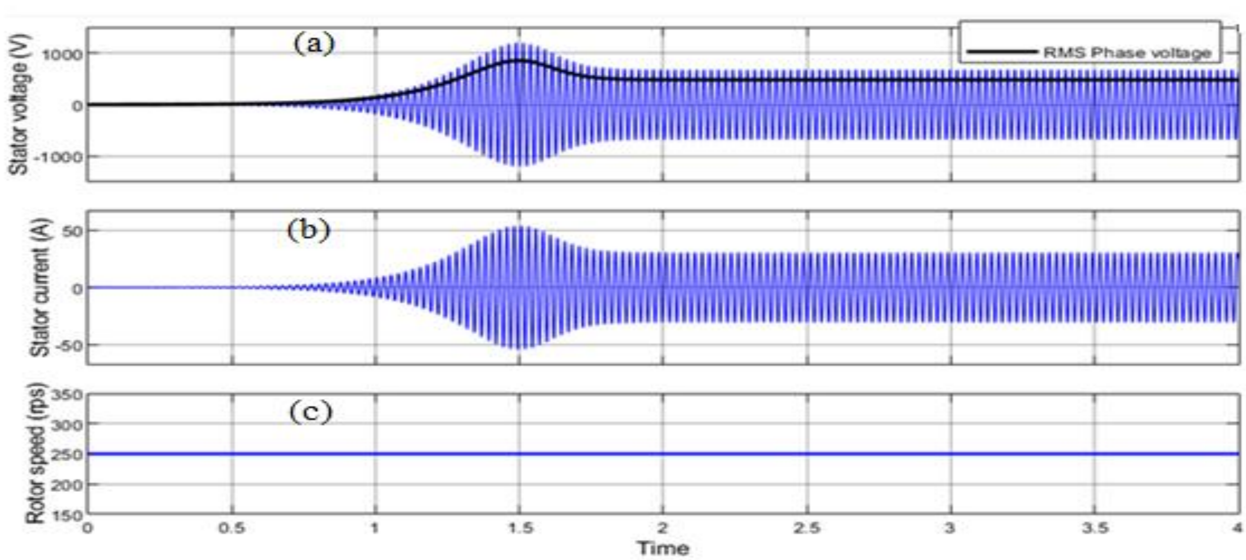

Figure 7: Excitation process at 180Uf capacitor and 250 rad/sec rotor speed (a) stator voltage (b) stator current (c) Machine speed.

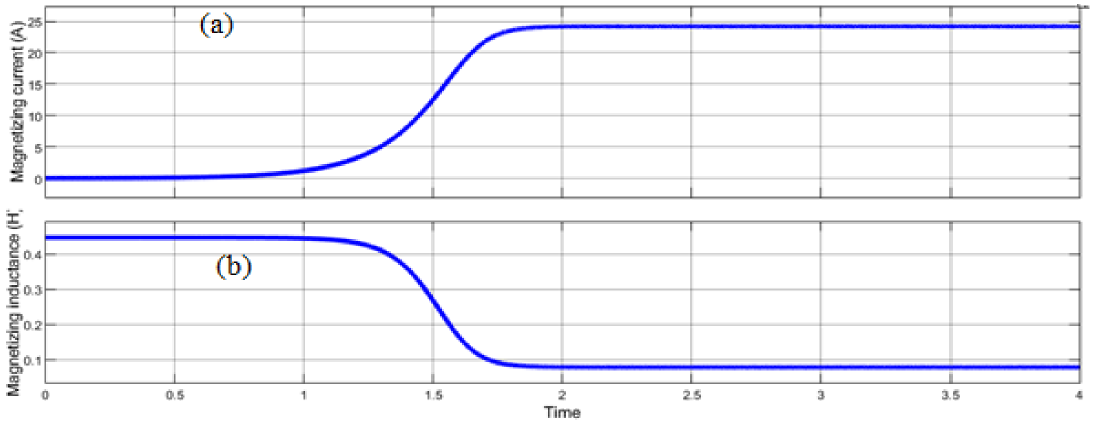

Figure 8: (a) Magnetizing current (b) Magnetizing inductance.

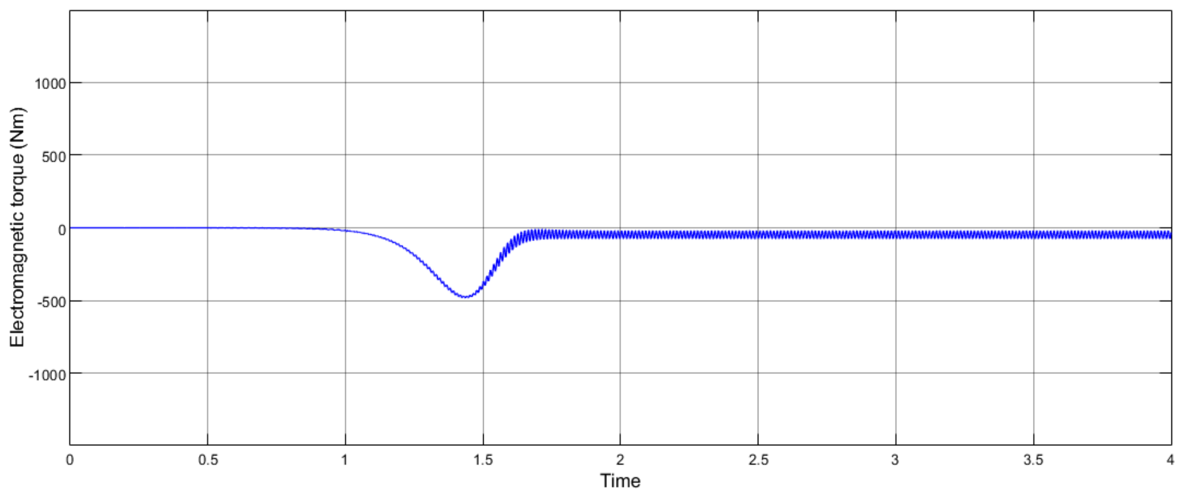

Figure 9: Electromagnetic torque vs. time.

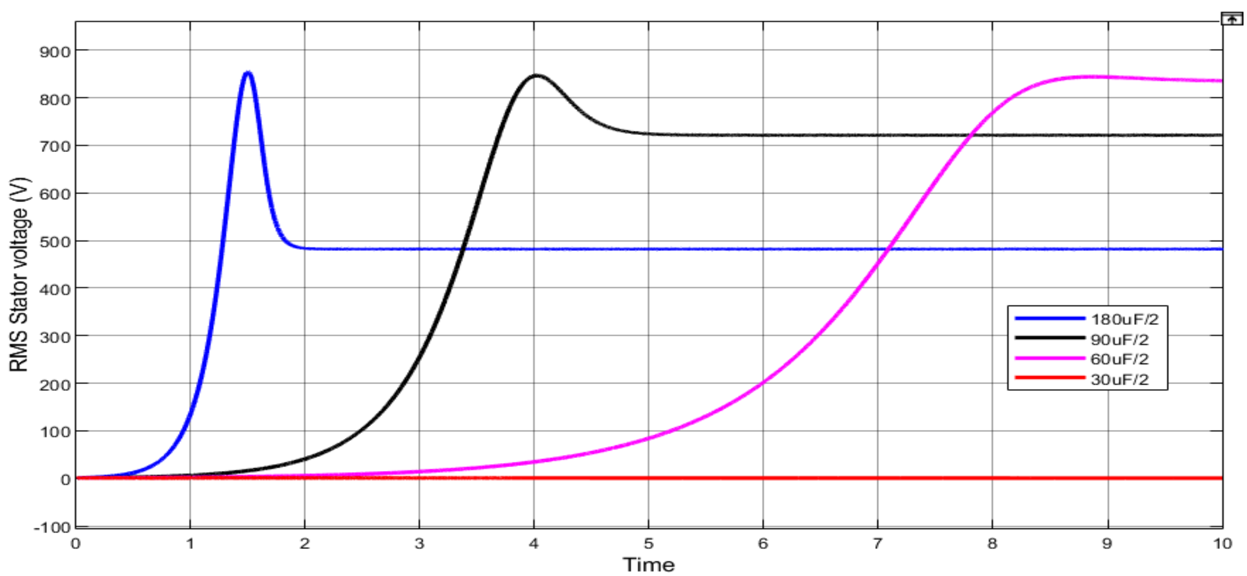

Figure 10: Voltage behavior of the SEIG under different excitation capacitance at 250 rad/sec.

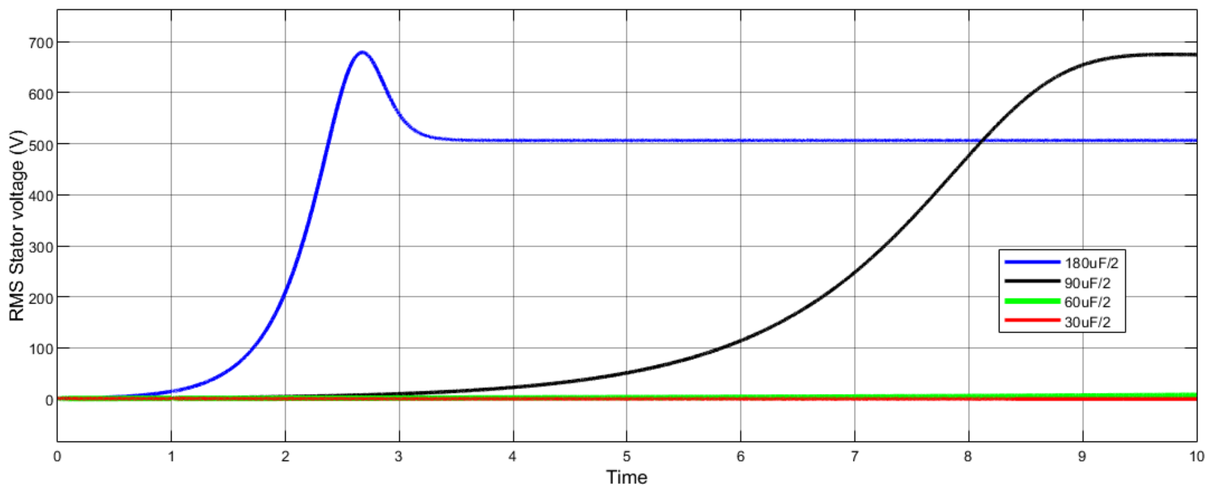

Figure 11: Voltage behavior of SEIG under different excitation capacitance at 200 rad/sec.

Figure 9 depicts the electromagnetic torque of SEIG. The negative value of electromagnetic torque is as a result of the negative slip which indicates that the induction machine is in the generating mode. Figure 10 illustrates the behavior of the machine with different values of excitation capacitance under the same rated speed (250 rad/sec). The simulation time was increased to 10s in order to be able to observe the steady state conditions.

Three important deduction can be made from the responses when $C = 180\mu F$, $90\mu F$ and$60\mu F$, these are; (i) there is an inverse relationship between the excitation capacitance and settling time of the phase voltage characteristics (ii) varying damping characteristics (iii) the steady state voltage increases as the excitation capacitance reduces. The main reason for this inverse relationship is the increase in the number of iterations performed before the stability condition is reached. When $C = 30\mu F$, voltage was not built up because saturation condition was not possible. In Figure 11, rotor speed was reduced to 200 rad/sec, and only excitation capacitance values $C = 180\mu F$ and $90\mu F$ were able to sustain voltage generation with both respectively showing underdamped (now with reduced overshoot) and overdamped characteristics.

IV. CONCLUSION

A comprehensive mathematical model of capacitive excited SEIG has been given. The need for the presence of remnant magnetic flux in the magnetic core has also been established as no self-excitation can be achieved without this. The results have shown that a non-suitable value of capacitor connected across the stator terminal of the asynchronous for a given speed would not be able to provide the necessary reactive power necessary for the excitation process and the steady state output of the generated voltage is not fixed but rather depends on the suitable combination of excitation capacitance, the rotor speed and magnetization characteristics. Output voltage characteristics of SEIG on load is not validated in this research.

NOMENCLATURE: All parameters are in standard units
w = rotating speed of an arbitrary reference frame
w_r =rotor electrical angular speed
C_d, C_q = dq -axis self-excitation capacitances
p =derivative operators
i_{ds}, i_{qs} =stator currents in the dq axis of the SEIG
i_{dr}, i_{qr} =rotor currents (referred to stator) in the dq axis of the SEIG
P =number of pairs of poles
T_L =load torque
K_{dr}, K_{qr} =initial rotational induced voltages along dq axis
i_m =magnetizing current
J =Moment of inertia
V_{ds}, V_{qs} =stator voltages in the dq-axis of the SEIG
V_{dsc}, V_{qsc} =dq stator capacitor voltage
V_{dr}, V_{qr} =rotor voltages (referred to stator) in the dq axis of the SEIG
V_{dsc0}, V_{qsc0} =initial dq capacitor voltages
L_{ls}, L_{lr} =stator and rotor (referred to stator) leakage inductances of SEIG
L_s, L_r =stator and rotor (referred to stator) self-inductances of SEIG
L_m =magnetizing inductance
r_s, r_r =stator and rotor (referred to stator) resistance of SEIG
$\lambda_{ds}, \lambda_{qs}$ =stator flux linkages in the dq axis of the SEIG
$\lambda_{dr}, \lambda_{qr}$ =rotor flux linkages in the dq axis of the SEIG
T_e =electromagnetic torque of the SEIG

REFERENCES

Al-Senaidi, S., A. Alolah, and M. Alkanhal, (2021). Parallel operation of three-phase self-excited induction generators with different numbers of poles. Engineering Science and Technology, an International Journal. 1-11.

Bassett, E., and Potter, F. (1935). Capacitive excitation for induction generators. Transactions of the American Institute of Electrical Engineers, 54(5), 540-545.

Bendjeddou, Y., A. Deboucha, L. Bentouhami, E. Merabet, and R. Abdessemed, (2021). Super twisting sliding mode approach applied to voltage orientated control of a stand-alone induction generator. Protection and Control of Modern Power Systems, 6(1): 1-9.

Debta, B. K. and Mohanty, K. (2010). Analysis on the effect of dynamic mutual inductance in voltage build-up of a stand-alone Brushless Asynchronous Generator. Engineering Science and Technology, an International Journal, 19(4): 1753-1762.

Goyal, S. K. and Palwalia, D. (2016). Analysis of performance parameters and estimation of optimum capacitance for asynchronous generator. Engineering Science and Technology, an International Journal, 19(4), 1753-1762.

Grantham, C.; D. Sutanto and B. Mismail. (1989). Steady-state and transient analysis of self-excited induction generators. Paper presented at the IEE Proceedings B (Electric Power Applications). 61-69.

Ion, B. and Syed, A. N. (2001). The Induction Machine Handbook (Electric Power Engineering Series): CRC press.

Mahato, S.; M. Sharma and S. Singh. (2006). Determination of minimum and maximum capacitances of a self-regulated self-excited single-phase induction generator using a three-phase winding. Paper presented at the 2006 India International Conference on Power Electronics. 28-33.

Mahato, S., Singh, S. and Sharma, M. (2013). Dynamic behavior of a single-phase self-excited induction generator using a three-phase machine feeding single-phase dynamic load. International Journal of Electrical Power & Energy Systems, 47, 1-12.

Ofualagba, G. and Ubeku, E. (2011). The analysis and modelling of a self-excited induction generator driven by a variable speed wind turbine. Fundamental and Advanced Topics in Wind Power, 5-9.

Ojo, O. and Bhat, I. (1995). An analysis of single-phase self-excited induction generators: model development and steady-state calculations. IEEE Transactions on Energy Conversion, 10(2), 254-260.

Seyoum, D. (2003). The dynamic analysis and control of a self-excited induction generator driven by a wind turbine: University of New South Wales. 120-210.

Seyoum, D. and Rahman, M. F. (2002). The dynamic characteristics of an isolated self-excited induction generator driven by a wind turbine. Paper presented at the Conference Record of the 2002 IEEE Industry Applications Conference. 37th IAS Annual Meeting (Cat. No. 02CH37344). 2: 731-738.

Silva, E. O.; W. E. Vanço and G. C. Guimarães. (2020). Capacitor bank sizing for squirrel cage induction generators operating in distributed systems. IEEE Access, 8, 27507-27515.

Simoes, M. G. and Farret, F. A. (2007). Alternative energy systems: design and analysis with induction generators (Vol. 13): CRC press.

Simões, M. G. and Farret, F. A. (2014). Modeling and analysis with induction generators: CRC Press.

Starkova,A. Y.; A. A. Chegodaev and R. R. Nasyrov. (2021). Prospects for distributed generation development in the Russian Federation. Paper presented at the 2021 3rd International Youth Conference on Radio Electronics, Electrical and Power Engineering (REEPE). 1-4.

Velmurugan, S.; R. Thenmozhi; P. Ramesh; R. Umamageswari; C. Bharatiraja and M. Kamalesh. (2021). FPGA collaborated one cycle control method in VSC for standalone self-excited induction generator. Materials Today: Proceedings, 45, 3100-3105.

Wang, Y. and Ossart, F. (2019). Simulation and Energy Management Interface of an Autonomous DC Microgrid. Paper presented at the 2019 IEEE 8th International Conference on Advanced Power System Automation and Protection (APAP). 1204-1208.

Wang, Z. and Madawala, U. K. (2021). A steady-state equivalent circuit of TSCAOI configured induction generator for renewable energy conversion systems. CPSS Transactions on Power Electronics and Applications, 6(1), 20-30.

Wu, B.; Y. Lang; N. Zargari and S. Kouro. (2011). Power conversion and control of wind energy systems (Vol. 76): John Wiley & Sons. 76: 49-200.